Energy efficiency for the removal of non-polar pollutants during ultraviolet irradiation, visible light photocatalysis and ozonation of a wastewater effluent

Please, cite using the citation below:

Javier Santiago-Morales, María José Gómez, Sonia Herrera-López, Amadeo R. Fernández-Alba, Eloy García-Calvo, Roberto Rosal, Energy efficiency for the removal of non-polar pollutants during ultraviolet irradiation, visible light photocatalysis and ozonation of a wastewater effluent, In Water Research, Volume 47, Issue 15, 2013, Pages 5546-5556, https://doi.org/10.1016/j.watres.2013.06.030.

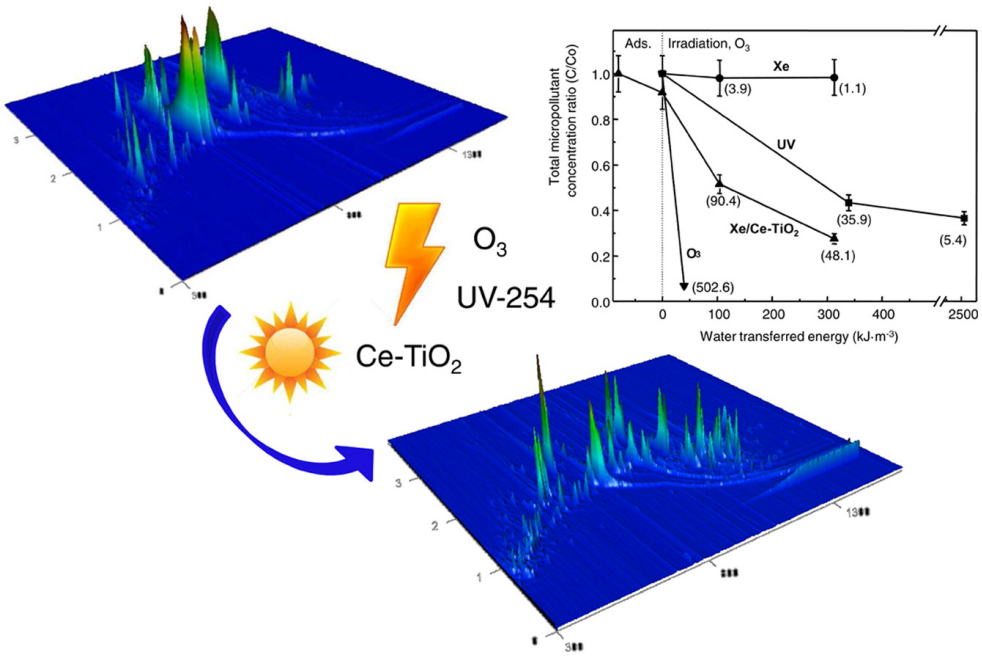

http://www.sciencedirect.com/science/article/pii/S0043135413005216

Energy efficiency for the removal of non-polar pollutants during ultraviolet irradiation, visible light photocatalysis and ozonation of a wastewater effluent

Javier Santiago-Morales[1], María José Gómez[2,3], Sonia Herrera-López[2,3], Amadeo R. Fernández-Alba[2,3], Eloy García-Calvo[1,2], Roberto Rosal[1,2,*]

[1] Department of Chemical Engineering, University of Alcalá, 28871 Alcalá de Henares, Madrid, Spain

[2] Advanced Study Institute of Madrid, IMDEA Agua, Parque Científico Tecnológico, 28805 Alcalá de Henares, Madrid, Spain.

[3] Pesticide Residue Research Group, Department of Hydrogeology and Analytical Chemistry, University of Almería, 04120, Spain.

* Corresponding author: roberto.rosal@uah.es

Abstract

This study aims to assess the removal of a set of non-polar pollutants in biologically treated wastewater using ozonation, ultraviolet (UV 254 nm low pressure mercury lamp) and visible light (Xe-arc lamp) irradiation as well as visible light photocatalysis using Ce-doped TiO_2. The compounds tracked include UV filters, synthetic musks, herbicides, insecticides, antiseptics and polyaromatic hydrocarbons. Raw wastewater and treated samples were analyzed using stir-bar sorptive extraction coupled with comprehensive two-dimensional gas chromatography (SBSE–CG x GC–TOF–MS). Ozone treatment could remove most pollutants with a global efficiency of over 95% for 209 μM ozone dosage. UV irradiation reduced the total concentration of the sixteen pollutants tested by an average of 63% with high removal of the sunscreen 2-ethylhexyl trans-4-methoxycinnamate (EHMC), the synthetic musk 7-acetyl-1,1,3,4,4,6-hexamethyltetrahydronaphthalene (tonalide, AHTN) and several herbicides. Visible light Ce-TiO_2 photocatalysis reached ~70% overall removal with particularly high efficiency for synthetic musks. In terms of power usage efficiency expressed as nmol kJ^{-1}, the results showed that ozonation was by far the most efficient process, ten-fold over Xe/Ce-TiO_2 visible light photocatalysis, the latter being in turn considerably more efficient than UV irradiation. In all cases the efficiency decreased along the treatments due to the lower reaction rate at lower pollutant concentration. The use of photocatalysis greatly improved the efficiency of visible light irradiation. The collector area per order decreased from 9.14 ± 5.11 m^2 m^{-3} $order^{-1}$ for visible light irradiation to 0.16 ± 0.03 m^2 m^{-3} $order^{-1}$ for Ce-TiO_2 photocatalysis. The toxicity of treated wastewater was assessed using the green alga *Pseudokirchneriella subcapitata*. Ozonation reduced the toxicity of treated wastewater, while UV irradiation and visible light photocatalysis limited by 20-25% the algal growth due to the accumulation of reaction by-products. Three transformation products were identified and tracked along the treatments.

Keywords: non-polar pollutants; ozonation; ultraviolet irradiation; visible light photocatalysis; energy efficiency.

1. Introduction

A wide variety of anthropogenic organic pollutants has been detected in surface waters during the last two decades. Most of them are pharmaceutical, personal care and household cleaning products, which, among others, constitute a new class of micropollutants usually referred to as emerging contaminants (Kümmerer, 2011). They are a result from human activities and are continuously released to the aquatic environment where their occurrence and concentration is quite variable depending on the proximity of urban or rural centres and their corresponding discharge points. In wastewater and receiving bodies they appear at concentrations in the ng/L to μg/L range (Rosal et al., 2010; Gómez et al., 2012). Most of them are not particularly toxic and due to their relatively low environmental concentration their risk has often been disregarded, but little attention has been paid to the formation of toxic transformation products. Some pollutants are regulated and a subject of increasing concern as they have, for example, been found in fish tissues above their Environmental Quality Standards (Miège et al., 2012). The establishment of these standards is a fundamental part of the environmental strategy of the European Union against water pollution in compliance with the Water Framework Directive (2000/60/EC of the European Parliament and Council) and other legal statutes (Decision 2455/2001/EC, Directive 2008/105/EC). The outcome is a list of substances endangering aquatic ecosystems, with the last proposal (Proposal COM 2011, 876 final, 31.1.2012) establishing 48 priority substances of which

21 are considered priority hazardous substances. It includes pesticides, biocides, chemicals, metals, polybrominated diphenyl ethers and polyaromatic hydrocarbons. Most emerging pollutants, such as pharmaceutical and personal care products, are not yet included in monitoring programs of the European Union although they could be future candidates due to the scientific consensus on their risk.

Current wastewater treatment plants (WWTP) are the main way of anthropogenic pollutants to enter the aquatic environment. Because of this continuous release of organic pollutants, their occurrence is becoming ubiquitous and might affect not only aquatic organisms but also endanger the reclamation of water in a moment when it appears as a chief strategy to fight against water scarcity. A suitable strategy could include an additional treatment after the biological process in order to remove contaminants and to improve surface water quality with respect to direct reuse (Muñoz et al., 2009). Several studies have noted that advanced oxidation processes (AOP) are an available technology that may successfully remove emerging and recalcitrant micropollutants from wastewater (Esplugas et al., 2007). AOP treatments are capable of generating highly oxidative species but they require chemicals, energy supply or both, and their energy efficiency is the subject matter of discussions (Katsoyiannis et al., 2011). It has also been shown that the formation of refractory by-products makes it difficult to achieve a high mineralization level (Krichevskaya et al., 2011). Moreover the degradation of the initial contaminants does not ensure any toxicity reduction target as transformation products can be even more toxic than their parent compounds (Shang et al., 2006; Santiago-Morales et al., 2013). There is a lack of investigations involving both energetic and ecotoxicity assessment as a step to allow its implementation in wastewater reuse scenarios using Life Cycle Assessment tools. Life cycle assessment is a well-known methodology to evaluate potential environmental impacts and has been previously proposed for water treatment processes (Zhang et al., 2010). The emissions to the aquatic environment should take into account aquatic ecotoxicity, whereas emissions to soil require the assessment of terrestrial and human ecotoxicity (Huijbregts et al., 2000). One of the limitations of this approach is the scarcity of information on the toxicity of treated samples and the difficulty of precisely establishing the required dosage of radiation or oxidants (Rodríguez et al., 2012).

In this study, we focused on the removal of non-polar micropollutants from biologically treated wastewater using irradiation and oxidation processes. Hydrophobic compounds pose an environmental threat because of their capacity to bioaccumulate in sediments and aquatic biota (Van der Oost et al., 2003). Also, the oxidative treatment of hydrophobic compounds produces oxidized transformation products with increased mobility (Santiago-Morales et al., 2012). The treatments studied were ozonation (O_3), ultraviolet (low pressure mercury lamp) and visible light (Xe-lamp) irradiation, the latter with and without photocatalyst (Ce/TiO_2). We analyzed treated samples with a method based on stir-bar sorptive extraction (SBSE) coupled with comprehensive two-dimensional gas chromatography (SBSE–CG x GC–TOF–MS) in order to track the most relevant non-polar pollutants in wastewater. SBSE–CG x GC–TOF–MS has been previously shown to display excellent results in the multianalysis of priority and emerging pollutants in water (Gómez et al., 2011). For all treatments, we followed the toxicity of treated samples for the green alga *Pseudokirchneriella subcapitata*.

2. Methodology

2.1 Materials

Wastewater was sampled from the secondary clarifier of a 3000 $m^3 h^{-1}$ WWTP placed in Alcalá de Henares, Madrid. This plant receives a mixture of domestic and industrial wastewater from industrial facilities located around the city. The biological treatment used a traditional A2O multistage configuration with nitrification-denitrification and enhanced phosphorus removal by phosphorus-accumulating microorganisms. The samples were stored in a refrigerator (< 4ºC) inside glass bottles and filtered using 0.45 μm glass fibre filters before runs and analyses. The samples of photocatalytic runs received an additional filtration at the end to remove the suspended catalyst. Table 1 shows the main wastewater parameters. All the analytical standards (purity >95%) included in this study were purchased from Sigma-Aldrich (Steinheim, Germany) or from Dr. Ehrenstorfer (Augsburg, Germany). Hydrochloric acid and sodium hydroxide (purity >95 %) used for pH adjustment were purchased from Sigma-Aldrich. The photocatalyst was a ceria-doped TiO_2 with 0.5 % wt, described in a previous work (Santiago Morales et al., 2012). It has a band gap of 2.63 eV, a surface area of 29 $m^2 g^{-1}$ and X-ray diffraction experiments showed that its crystallographic phase corresponds to anatase crystals. The catalyst suspended in wastewater displayed a ζ-potential of 16.7 ± 0.8 mV and a mean particle size of 547 ± 33 nm determined by dynamic light scattering (DLS).

2.2. Experimental setup and procedure

The irradiation experiments used a Heraeus TQ Xe 150 Xe-arc lamp with spectral emission in the visible region and 15 W Heraeus Noblelight TNN 15/32 low-pressure mercury vapour lamp (UV) emitting at 254 nm. The lamps were placed inside a quartz jacketed sleeve refrigerated using a thermostatic bath. The reaction temperature was closely controlled at 25ºC in all cases. For visible light irradiations an additional borosilicate glass tube was used to absorb wavelengths < 290 nm. Fluence rates per unit volume were 6.01 x 10^{-6} E L^{-1} s^{-1} (254 nm) for the UV lamp and 1.05 x 10^{-6} E L^{-1} s^{-1} (290-400 nm) for the Xe-arc lamp. The chemical actinometers

Table 1. Analysis of wastewater (TSS = Total suspended solids, NPOC = Non-purgeable organic carbon, COD = Chemical oxygen demand, SUVA-254 = Specific ultraviolet absorbance at 254 nm)

pH	7.8 (in situ)
Dissolved oxygen (mg L^{-1})	8.7 (in situ)
TSS (mg L^{-1})	20 (as received)
Turbidity (NTU)	2.5
Conductivity (μS cm^{-1})	875
NPOC (mg L^{-1})	8.1
COD (mg L^{-1})	28
Hardness (mg $CaCO_3$ L^{-1})	219
N-NO_3 (mg L^{-1})	9.8
SUVA-254 (L mg^{-1} m^{-1})	1.7
Anions and cations (mg L^{-1})	
Sulphate	79.9
Chloride	80.6
Phosphate	2.6
Potassium	14.9
Magnesium	21.6
Calcium	52.2
Sodium	70.5
Metals (μg L^{-1})	
Chromium	13
Nickel	12.3
Cobalt	1.8
Strontium	560
Copper	1.7
Tin	0.29
Lead	0.49
Titanium	0.93
Manganese	0.92
Vanadium	1.1
Molybdenum	4.3
Zinc	34
Micropollutants (ng/L)	
2-Ethylhexyl trans-4-methoxycinnamate (EHMC)	23.6 ± 8.1
Oxybenzone	14.4 ± 1.7
1,3,4,6,7,8-hexahydro-4,6,6,7,8,8-hexamethylcyclopenta(g)-2-benzopyran, Galaxolide (HHBC)	4212 ± 340
Musk ketone	84.9 ± 6.7
7-acetyl-1,1,3,4,4,6-hexamethyltetrahydronaphthalene, Gonalide (AHTN)	461.3 ± 32.7
Butyl hydroxytoluene (BHT)	164.6 ± 24.4
Atrazine	183.5 ± 9.6
Metolachlor	208.4 ± 31.4
Terbutryn	8.3 ± 1.8
Terbuthylazine	5.5 ± 0.8
Chlorpyrifos-ethyl	2.4 ± 0.4
Diazinon	59.5 ± 11.0
Clorophene	3.6 ± 1.4
Triclosan	101.2 ± 20.6
Phenanthrene	2.5 ± 0.6
Pyrene	1.4 ± 0.3

used were hydrogen peroxide and 2-nitrobenzaldehyde, which allowed us to obtain the indicated values for the UV and Xe lamps, respectively (Nicole et al., 1990; Allen et al., 2000).

Ozone was continuously bubbled during the run from a corona discharge ozone generator with a gas flow of 0.19 Nm^3 h^{-1} and concentration of ozone of 22 g Nm^{-3}. The ozone dosage, O_D, was determined, from the integration of the ozone absorption rate equation:

$$O_D(t) = E\, k_L a \left(C^*_{O_3}\, t - \int_0^t C_{O_3}\, dt \right) \qquad (1)$$

where $C^*_{O_3}$ is equilibrium concentration of dissolved ozone and k_La the volumetric mass transfer coefficient. The enhancement factor, E, can be estimated from Hatta number as indicated in a previous work (Rosal et al., 2010). Details on the experimental methodology can be found elsewhere (Rosal et al., 2008). All experiments were performed in batch mode in a 1.3 L vessel magnetically stirred at 900 min^{-1} and the samples were withdrawn at prescribed intervals for analyses. To remove dissolved ozone from the samples we used nitrogen bubbling. This method avoids chemical quenchers and for the experimental conditions used it has been verified that the concentration of dissolved ozone falls below 3% in less than 30 s (Rosal et al., 2010). Throughout all the experiments pH was kept at 7.5 ± 0.1 units. The catalyst was used at a concentration of 200 mg L^{-1} and stirred for 30 min before each run to ensure surface charge equilibration. The concentration of dissolved oxygen throughout photocatalytic treatments was 31-33 mg/L kept by constant oxygen bubbling.

2.3. Analyses

The analyses of micropollutants were performed using stir bar sorptive extraction (SBSE) coupled with comprehensive two dimensional gas chromatography (GC x GC–TOF–MS). This technique allows the simultaneous separation and determination of difficult to resolve constituents in complex mixtures at very low concentrations. This technique is based on the use of 20 mm (length) x 0.5 mm (film thickness) PDMS commercial stir bars (Gerstel, Muelheim an der Ruhr, Germany) loaded overnight and subsequently desorbed in a thermal desorption unit (Gerstel) connected to a programmed temperature vaporization (PTV) system injector CIS-4 (Gerstel) by a heated transfer line at 300 ºC. The PTV injector was placed in a GC x GC–TOF–MS system Agilent 7890A gas chromatograph equipped with an additional oven and a quad-jets modulator (two cold jets and two hot jets). Liquid nitrogen used for cooling was automatically delivered from a 60 L Dewar liquid nitrogen storage tank. The first column (non-polar) was a 10 m x 0.18 mm i.d., 0.2 mm film thickness Rtx-5 coated with 5% diphenyl 95% dimethylpolysiloxane (Restek). The second column (semipolar) was a 1 m x 0.1 mm i.d., 0.10 mm film thickness Rxi-17 coated with 50%

diphenyl 50% dimethylpolysiloxane (Restek). The MS system was a Pegasus 4D TOF (LECO Corporation). The method detection limits (MDLs) and method quantification limits (MQLs) in wastewater of the compounds analyzed in this study ranged between 0.02 to 3.07 ngL^{-1} and 0.06 to 10.23 ngL^{-1} respectively. Sample preparation details of the analytical method as well as the performance might be obtained elsewhere (Gómez et al., 2011).

A Metrohm 861 Advance Compact IC with suppressed conductivity detector allowed quantifying cations using a Metrosep C3 column with 5.0 mM HNO_3 eluent at 1 mL min^{-1}. Anions were determined in the same equipment using a Metrosep A Supp 7-250 analytical column with 36 mM Na_2CO_3 as eluent at 0.8 mL min^{-1}. Non Purgeable Organic Carbon (NPOC) was analyzed in a Shimadzu TOC-VCSH total carbon organic analyzer. Absorbance measurements were performed in a Shimadzu UV-1800 spectrophotometer. Trace metals were quantified by Inductively Coupled Plasma-Mass Spectrometry using a quadrupole mass spectrometer Agilent 7700X operating at 3 MHz in helium cell gas mode. The concentration of ozone dissolved in the aqueous phase was measured with an amperometric Mettler Toledo 358/210 dissolved ozone sensor calibrated using the Indigo Colorimetric Method (SM 4500-O3 B). The signal was transmitted to a Mettler Toledo Thornton M300 and finally monitored and recorded using an Agilent 34970 Data Acquisition Unit connected to a computer. The concentration of ozone in gas phase was determined using an Anseros Ozomat GM6000 Pro photometer calibrated against potassium iodide. The BET specific surface was evaluated by nitrogen adsorption at 77 K using an SA 3100 Beckman Coulter Analyzer. The catalyst was characterized by X-ray diffraction (XRD) using a Seifert 3000P diffractometer (Cu Kα, λ = 1.5406 Å). DLS measurements were conducted in Malvern Zetasizer Nano ZS equipment. ζ-potential was measured via electrophoretic light scattering combined with phase analysis light scattering in the same instrument.

The toxicity of partially oxidized mixtures was assessed using the multigenerational growth inhibition of the green alga *Pseudokirchneriella subcapitata* according to OECD TG 201 (OECD, 2011). Algae were cultured in OECD growth medium at pH adjusted to 8.0 ± 0.2. A culture kept in 25 mL agitated flasks was inoculated three days before each test. The exposed cultures were kept in 96-well clear microplates with a total dosed volume of 210 μL, each well containing 180 μL of sample, 20 μL of a concentrated OECD growth medium and 10 μL of microalgae. During 72 h algae were grown in a chamber under continuous fluorescent illumination of 100 μE m^{-2} s^{-1} at 22 ºC. The chlorophyll content was measured daily by fluorescence (Excitation 444nm – Emission 680 nm) using a Fluoroskan Ascent FL plate fluorometer-luminometer as substitute parameter for algal biomass production.

3. Results and discussion

3.1. Removal of micropollutants

We detected and quantified 16 micropollutants in the wastewater samples. The list includes 6 personal care products, namely the UV filters 2-ethylhexyl trans-4-methoxycinnamate (EHMC) and oxybenzone, the synthetic musks 1,3,4,6,7,8-hexahydro-4,6,6,7,8,8-hexamethylcyclopenta(g)-2-benzopyran (galaxolide, HHBC), 7-acetyl-1,1,3,4,4,6-hexamethyltetrahydronaphthalene (tonalide, AHTN) and musk ketone and the food additive (antioxidant) butyl hydroxitoluene (BHT). We also detected 8 pesticides/biocides and 2 polycyclic aromatic hydrocarbons (PAH): atrazine, metolachlor, terbutryn, terbuthylazine, chlorpyrifos-ethyl, diazinon, chlorophene, triclosan, phenanthrene and pyrene (Table 1). It is interesting to note that atrazine and metolachlor are excluded from of EC Regulation 1107/2009 (or the former Annex I of Council Directive 91/414/EEC). The abundance of HHBC and AHTN in treated wastewater complies with data published elsewhere and it is due to their very large consumption incorporated in a wide variety of personal care products in which they act as a fragrance fixative (Santiago-Morales et al., 2012). The other contaminants analyzed with concentrations in the order of hundreds of ng L^{-1} were the herbicides atrazine and metolachlor, frequently used in the past in gardening, the antioxidant additive BHT, and the antiseptic triclosan, included in a number of personal care products such as toothpastes.

The results of the irradiation and ozonation treatments on these pollutants are shown in (Table 2). Ozone was capable of removing most of the analyzed pollutants, particularly HHBC, AHTN and all the pesticides, with a global efficiency of +95% for an ozone dosage (calculated according to Eq. 1) of 209 ± 38 μM. The data for HHBC (97% removal) showed a higher degradation than found by Rosal et al. (2010) who encountered 83% removal for 340 μM ozone dosage. This could be explained by a lower COD for the wastewater used in this work. Snyder et al. (2006) observed 80-90% removal for HHBC in river water and in WWTP effluents using ozone dosages comparable to that of this work. It is interesting to note that EHMC and musk ketone were not significantly removed by ozone. This is in good agreement with data reported elsewhere: for the ozonation of musk ketone Rosal et al (2010) reported no degradation for 220 mM ozone dosage whereas Snyder et al. (2006) found depletions of <1 % and 17% for low and high ozone dosages, respectively. Triclosan was almost completely removed by ozone while pyrene fell below its quantification limit. UV irradiation reduced the total concentration of the sixteen pollutants tested by an average of 63%. A remarkable fact is that musk ketone and EHMC were removed up to 92% and 50% respectively after 15 min, with substantial degradation taking place during the first 2 min (Table 2). 254 nm UV

Table 2. Removal of pollutants for irradiation, photocatalytic and ozonation treatments (expressed as $c(t)/c_o$). Reaction conditions: UV used a 15W low pressure mercury lamp with fluence rate 6.01 x 10^{-6} E L^{-1} s^{-1} (254 nm); Xe and Xe-TiO_2 used a Heraeus TQ Xe 150 Xe-arc lamp with fluence rate 1.05 x 10^{-6} E L^{-1} s^{-1} (290-400 nm); the catalyst concentration was 200 mg/L; ozone gas flow and concentration were 0.19 N m^3 h^{-1} and 22 g Nm^{-3}.

		UV		Xe		Xe/Ce-TiO_2		O_3
No.	Compound	2 min	15 min	2 min	15 min	2 min	15 min	22 min
1	EHMC	0.38	0.50	0.94	0.77	1.00	0.87	1.00
2	Oxybenzone	0.70	0.52	1.08	1.01	1.00	1.07	0.75
3	Galaxolide (HHBC)	0.47	0.46	1.00	1.01	0.53	0.22	0.03
4	Musk ketone	0.60	0.08	1.00	0.84	0.49	0.36	1.10
5	Tonalide (AHTN)	0.12	0.02	0.85	0.99	0.31	0.15	0.02
6	BHT	0.34	0.26	1.02	0.50	0.72	0.40	0.34
7	Atrazine	0.48	< 0.02	0.91	1.00	0.82	0.85	< 0.02
8	Metolachlor	0.37	0.003	0.94	1.00	0.67	0.72	< 0.002
9	Terbutryn	0.23	< 0.02	1.08	1.07	0.54	0.22	< 0.02
10	Terbuthylazine	0.43	< 0.10	0.94	0.91	0.74	0.68	< 0.10
11	Chlorpyrifos-ethyl	0.86	0.63	1.00	1.10	0.67	0.25	< 0.17
12	Diazinon	0.82	0.04	0.96	0.93	1.02	1.01	< 0.002
13	Chlorophene	< 0.02	< 0.02	0.81	0.86	0.85	0.72	< 0.02
14	Triclosan	0.03	0.02	1.17	0.90	0.63	0.47	0.02
15	Pyrene	0.67	0.52	1.06	0.99	1.09	1.00	< 0.06

irradiation also resulted in high removal efficiencies for AHTN, atrazine, metolachlor, terbutryn, diazinon, chlorophene and triclosan (all of which were removed +99% in 15 min).

The rate of photolysis of a given compound at any concentration, c_P, can be calculated assuming for the photoreactor the model of linear source with emission in planes parallel to the lamp axis (LSPP). Details on the derivation can be found elsewhere (Beltrán, 2003):

$$-\frac{d\,c_P}{dt} = F_P \Phi_P \frac{2\pi R_o L E_o^{'}}{V}\left[1 - e^{-\mu(R_1 - R_o)}\right] \qquad (2)$$

μ is the attenuation coefficient and F_p the fraction of the absorbed radiation absorbed by a given compound, P:

$$\mu = 2.303 \sum \varepsilon_i\, c_i \qquad (3)$$

$$F_P = \frac{\varepsilon_P\, c_P}{\sum \varepsilon_i\, c_i} \qquad (4)$$

Φ_P is the quantum yield, R_o the inner radius of the photoreactor, L the length of the lamp, V the irradiated volume, $E_o^{'}$ the fluence rate at R_o (expressed in W cm^{-2}) and ε_P and ε_i the molar extinction coefficients of compound P and a generic compound in the mixture. Using the experimental values of $\Sigma\, \varepsilon_i\, c_i = 0.137$ cm^{-1} and $(R_1\text{-}R_o) = 2.58$ cm, the value for μ $(R_1\text{-}R_o)$ was 0.814, constant throughout the runs because the absorbance of wastewater (and the attenuation coefficient) did not change appreciably during treatments. In what follows, the initial value for F_p was used for integrating Eq. 2 to get the concentration of irradiated compounds as a function of volume based fluence ratio, $E_{Vo}^{'}$ (expressed in W m^{-3}):

$$\frac{c_o - c_P}{t} = k = F_P \Phi_P E_{Vo}^{'}\left[1 - e^{-\mu(R_1 - R_o)}\right] \qquad (5)$$

where k is the rate constant in mol L^{-1} min^{-1}. The two sides of Eq. 3 were plotted for each micropollutant for which quantum yields and molar extinction coefficients were available (See Table S2 in Supporting Information). The results are displayed in Fig. 1 in which the dashed line indicates the theoretical degradation rates obtained from Eq. 3. The points located below this line represent compounds with experimental rate constants lower than those theoretically calculated using their specific absorbance and quantum yield. The opposite stands for values above the theoretical line. The graph shows that all pollutants disappeared at rates close to their theoretical values with experimental values slightly overestimated by theoretical calculations. This drift is most probably due to a decrease in F_p during irradiation. For compounds with a degradation rate above theoretical prediction (oxybenzone and chlorpyrifos-ethyl) other degradation mechanisms could be involved such as the reaction with hydroxyl radicals generated by photolysis of nitrate and nitrite or the photosensitization by dissolved organic matter (Mack and Bolton, 1999; Werner et al., 2005).

Visible light Xe-lamp driven photolysis led to a reduced removal of micropollutants, with an average of 1.4% for those tested in this work. However, visible light

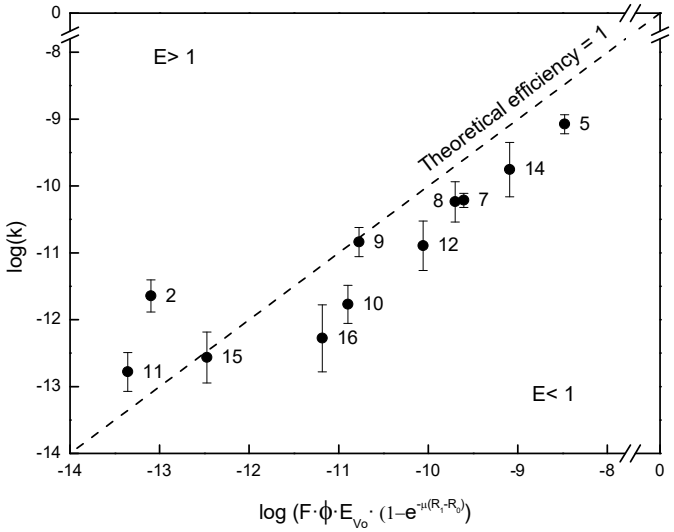

Figure 1. First-order constant rate for micropollutant removal during UV irradiation as a function of their theoretical rate of photolysis (Eq. 4). For compound identification see Table 2.

irradiation (filtered from wavelengths < 290 nm) was able to reduce the concentration of 4 (of 16)micropollutants in the 14-50% range. Remarkably, BHT became depleted by 50%. EHMC and musk ketone also displayed relatively high removal rates with depletion percentages in the 20% range after only 15 min of irradiation. These data indicate the relevance of natural irradiation in the environmental degradation of these pollutants.

Visible light Ce-TiO_2 photocatalysis was much more efficient and reached ~70% overall removal after 15 minutes. The main contribution was the high removal efficiency observed for the synthetic musks HHBC, AHTN and musk ketone (in the 64-85% range). Some other compounds, like oxybenzone, diazinon and the two polyaromatic hydrocarbons (phenanthrene and pyrene) did not suffer any significant degradation. Fig. 2 displays the photocatalytic removal efficiency of the tested micropollutants as a function of their octanol-water partition coefficient, K_{ow} (Table S1). (Because all compounds are non-polar, their dissociation constants are not significant for calculating the octanol-water partition coefficient.) For a group of pollutants, located in the shadowed region of Fig. 2, there is a clear relationship between photocatalytic removal efficiency and K_{ow}. Another group of five compounds showed no degradation or very low removal ratios (< 15%), namely EHMC, oxybenzone, diazinon, phenanthrene and pyrene. The insert of Fig. 2 also includes the percentage of dark adsorption taking place before irradiation. Diazinon (12) significantly adsorbed on the surface of the Ce-TiO_2 catalyst probably due to its positive charge at the pH of wastewater, which would allow electrostatic interaction with the deprotonated catalyst surface. The surface interaction of chlorophene (13), adsorbing > 20%, was most probably due to the electroneutral interaction with the separated proton in the proximity of TiO_2 surface (Friedmann et al., 2010). D'Oliveira et al. (1993) encountered a linear relationship between apparent first-order rate constants, Hammett constants and octanol-water partition coefficients for several chlorophenols during TiO_2 photocatalysis. In their work, K_{ow} showed a positive correlation with apparent rate constants, a similar behaviour as that reported here. The same result was indicated for several pesticides by Tanaka and Reddy (2002). All these findings suggest that photocatalytic degradation of non-polar compounds might be mainly governed by the adsorption on the catalyst surface. The indirect reaction, which takes place by mediation of photogenerated radical species with soluble compounds, would be less efficient in this case than hole-based oxidation.

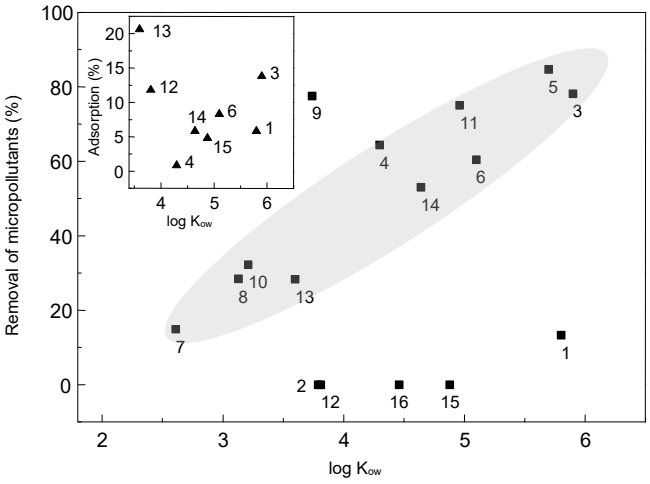

Figure 2. Photocatalytic removal of micropollutants as a function of the apparent octanol-water partition coefficient, K_{ow}. Insert: pollutant adsorption on catalyst surface for photocatalytic runs. The numbers refer to compounds as listed in Table 2.

It is interesting to note that the depletion of the tested organic compounds by ozone is not directly related to the second order direct or indirect ozonation rate constants (See Table S2). There are several reasons for it derived from the intrinsic complexity of ozonation reactions. First, ozonation is a heterogeneous process, which takes part not only in the bulk, but also at the gas-liquid interface. Moreover, at the beginning of run there was no ozone in solution, and then the reactions took place at the gas-liquid interface or within the liquid film. Non-polar organics tend to accumulate at the surface, while more polar or dissociated compounds remain in the bulk, thus there is a preferential reactivity of the former during the first minutes. The fact that compounds with similar reaction rate became depleted at very different actual rates depending on their polarity has already been observed in a previous work (Rosal et al., 2010). Ozonation can be a direct reaction or hydroxyl radical-mediated process in which the availability of hydroxyl radicals determines the governing path. Radical reactions are highly influenced by the presence of interfering compounds. For example, it has been demonstrated that the reaction of aromatic compounds with hydroxyl radical is inhibited by dissolved natural organic matter,

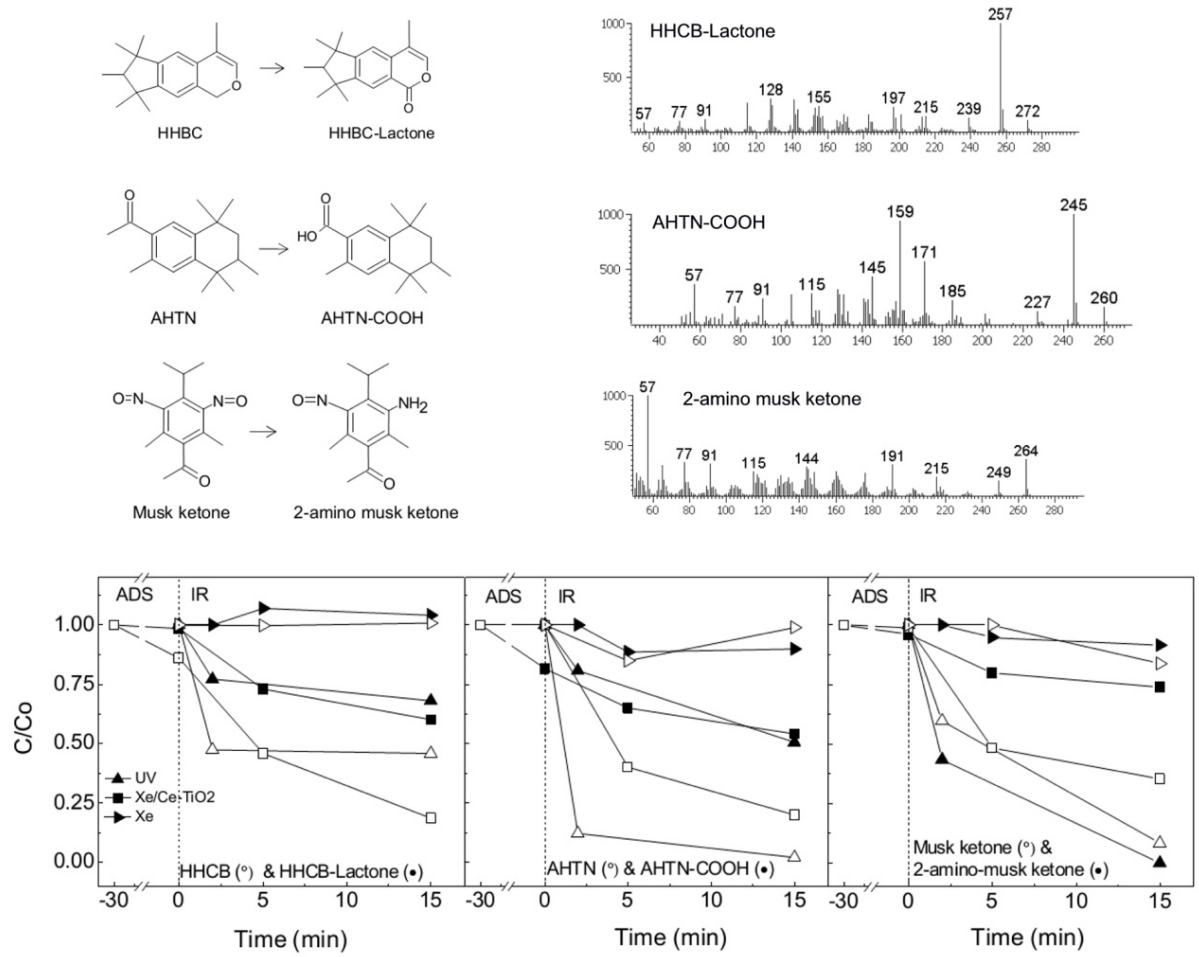

Figure 3. Concentration profile for the photodegradation of AHTN, HHCB and musk ketone, shown by empty symbols, and its main transformation products, HHCB-Lactone, AHTN-COOH and 2-amino musk ketone displayed with filled symbols. (ADS: adsorption, IR: irradiation.) The upper part of the figure shows the mass spectra identification of HHCB-Lactone, AHTN-COOH and 2-amino musk ketone.

the probable reason being that hydroxyl radical formation occurs in micro-environmental sites remote from the aromatic compounds (Lindsey and Tarr, 2000). Moreover, the partition coefficient of a hydrophobic compound to dissolved organic matter also plays a significant role, up to the point that the presence of natural organic matter dramatically hinders the degradation of hydrophobic compounds even at too low concentrations to significantly scavenge hydroxyl radicals.

Besides the depletion of the compounds shown in Tables 1 and 2, we also tracked three relevant metabolites of three of them, namely HHBC-lactone from HHBC, AHTN-COOH (3,5,5,6,8,8-hexamethyl-5,6,7,8-tetrahydronaphthalene-2-carboxylic acid) from AHTN and 2-amino musk ketone from musk ketone. They were identified by GC x GC-TOF-MS and their concentrations during irradiation are displayed in Fig. 3 for irradiation runs. AHTN-COOH and 2-amino musk ketone were tentatively assigned according to mass spectra found in the literature (Valdersnes et al., 2006; Gatermann et al., 1998). HHBC-lactone is a biotransformation product of HHBC produced in WWTP operating with activated sludge (Bester, 2004). Apart from its biological origin, HHBC-lactone is a component of technical HHBC and was identified in river water samples at a comparable concentration or even higher than those for HHBC (Gómez et al., 2012). We also detected 2-amino musk ketone at levels higher than those of its parent compound. 2-amino musk ketone is the most common metabolite of musk ketone and is a suspected endocrine disruptor able to interact with oestrogen receptors (Champagne, 2008). AHTN-COOH has recently been shown to come out from AHTN reaction with sodium hypochlorite as a disinfection by-product (Kuhlich et al., 2011). The concentration of the three transformation products were significantly reduced by UV irradiation, particularly that of 2-amino musk ketone, which disappeared completely after 15 min. Xe/Ce-TiO_2 reached removal efficiencies within 25-50%, while visible light irradiation did not induce any significant depletion. Fig. 3 also shows the depletion of HHBC, AHTN and musk ketone during UV, Xe and Xe/Ce-TiO_2 irradiation processes. Concerning ozonation runs, the more polar character of TP and their higher removal rates make them more difficult to be

detected and quantified. The identification of TP from galaxolide has been recently considered in detail in a recent paper in which we used liquid chromatography/hybrid quadrupole time-of-flight mass spectrometry (Herrera et al., 2013). In this work we could detect HHCB-lactone in ozonated samples because its concentration was relatively high (103 ng/L). In a previous research we showed that during the first minutes of ozonation, HHBC-lactone could increase because it is also a transformation product formed during the ozone treatment of HHCB (Santiago-Morales et al., 2012). In this work, we obtained > 98% removal of HHBC-lactone after 22 min on stream. Pure irradiation treatments (UV, Xe) did not lead to any significant removal of the organic carbon initially present in the wastewater sample while Xe/Ce-TiO_2 photocatalysis reduced the amount of dissolved carbon 9% after 15 min. Ozonation led to a maximum mineralization of 40%, with NPOC removal below 15% after 15 min on stream. Moderate TOC removal is typical for most practical forms of AOP and favours the formation of organic transformation products, giving way to more complex reaction mixtures. In similar conditions we reported several cases of enhanced toxicity for aquatic organisms (Rosal et al., 2009; Gómez-Ramos et al., 2011).

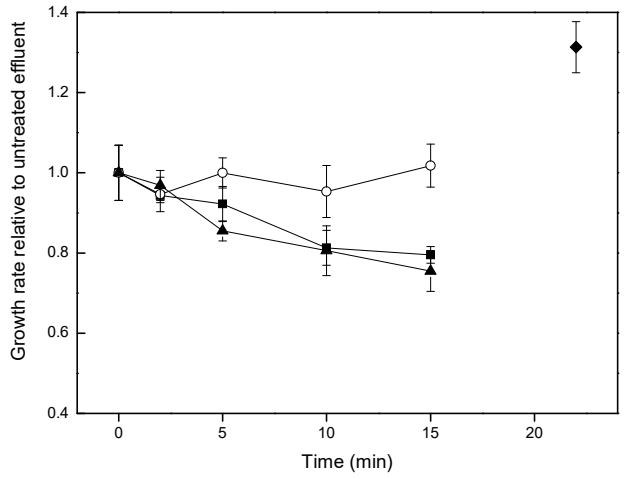

Figure 4. Toxicity of irradiated and ozonated wastewater samples. Ozonation (◆), UV (■), Xe (○), Xe/Ce-TiO_2 (▲).

The toxicity of treated samples for the green algae are displayed in Fig. 4 expressed as growth rate relative to untreated wastewater. Ozonation was the only treatment that could reduce the toxicity with respect to raw wastewater. The UV irradiation and Xe/Ce-TiO_2 visible light photocatalysis led to a growth rate reduction of up to 20-25% after 15 min of irradiation. The plot in Fig. 4 is accompanied with 95% confidence intervals, which show significant toxic responses at least after 5 min, while pure visible light irradiation has no effect at all. The enhancement in wastewater toxicity during irradiation processes is most probably due to the generation of transformation products that may be more toxic than the parent ones. It is interesting to note that UV and Xe irradiation did not reduce NPOC and that for Xe/Ce-TiO_2 the reduction was only 9%, a modest figure in comparison with the ozone treatment which reached NPOC removal of 40%. Additionally, synergistic effects between mixture components might make favour toxic responses in complex mixtures. The generation of a high number of transformation products from every single parent pollutant would be a cause for concern (Boltes et al., 2012; Santiago-Morales et al., 2013).

UV and visible light irradiation treatments are initially quite different, but the similar generation of TP and the comparable toxicity pattern suggest a deeper analogy. During UV irradiation at 254 nm, it is expected a certain oxidative contribution from hydroxyl radicals originated during the photolysis of nitrate (Lam et al., 2003). Also, from water photolysis as the low-pressure mercury lamp used in this work yielded about 5% of its total power at 185 nm, in the vacuum UV. Visible light photocatalysis may also generate hydroxyl radicals by catalyst photoexcitation even though the direct oxidation on catalyst holes would eventually dominate. The lower capacity of irradiation processes to generate highly oxidant species would be the underlying reason for the main differences observed.

3.2. Energy efficiency

Water transferred power (*WTP*, expressed in W m^{-3}) was used to quantify the amount of energy entering a volume of water per unit time. The energy could be supplied in several forms such as radiation, electricity, or chemical energy. For irradiation processes, *WTP* was obtained from the fluence rate, $E_o^{'}$, the irradiated area *A* and the volume of treated water *V*:

$$WTP = \frac{E_o^{'} A}{V} \quad (6)$$

For ozonation, *WTP* was calculated using standard enthalpy of formation of O_3 to convert ozone dosage into chemical energy:

$$WTP_{O_3} = \frac{F C \Delta H}{V} \quad (7)$$

F is the gas flow ($Nm^3 s^{-1}$), C the $O_3(g)$ concentration (g Nm^{-3}), ΔH the formation enthalpy of ozone (2.97 kJ g^{-1}) and *V* the volume of treated water. The results of *WTP* for the irradiation and ozonation processes used in this work are listed in Table 3. It is interesting to note that UV irradiation supplied one and two orders of magnitude more power than visible light irradiation and ozonation respectively. For the derivation of Table 3 we assumed gas-to-liquid ozone transfer efficiency of 75% as discussed elsewhere (Muñoz et al., 2009). The energy transferred to treated water, *WTE* is *WTP* multiplied by time. Fig. 5 shows the influence of the water transferred energy *WTE* (kJ m^{-3}) for photochemical and oxidation treatments on the depletion of total micropollutant concentration. Ozonation was by far the most efficient treatment in terms of the amount of micropollutants

removed per unit of energy transferred to the water. The sample used for ozone treatments was taken once ozone appeared in solution and reasonably reached a plateau. This choice represents an ozone dosage not much higher than that required for rapid direct ozone reactions to complete and would be a reasonable minimum ozone dosage for wastewater treatment.

Table 3. Water-transferred power (WTP), electrical energy per order (E_{EO}) collector area per order (A_{CO}) for the different treatments

Treatment	WTP (W m^{-3})
UV irradiation (254 nm)	2828
Visible light irradiation (Xe lamp 290-400 nm)	348
Ozonation[a]	29.5
E_{EO} (kWh m^{-3} $order^{-1}$)	
UV irradiation (254 nm)	2.56 ± 1.85
Ozonation[a]	0.18
A_{CO} (m^2 m^{-3} $order^{-1}$)	
Visible light irradiation (Xe lamp 290-400 nm)	9.14 ± 5.11
Xe/Ce-TiO_2 photocatalysis	0.16 ± 0.03

a) Assuming gas-to-liquid ozone transfer efficiency of 75% (Muñoz et al., 2009).

Photocatalytic Xe/Ce-TiO_2 required considerably lower energy than UV to remove the same amount of micropollutants. The contribution of dark adsorption on catalyst surface to pollutant depletion (~10%) is also shown in Fig. 5. As indicated before, the non-catalytic degradation by visible light resulted negligible.

The efficiency of energy usage can be quantified using the concept of transferred energy efficiency (*TEE*). *TEE* (nmol kJ^{-1}) is the ratio between concentration removal of micropollutants (nmol L^{-1}) and *WTE*. A higher value means better energy usage efficiency. The values of *TEE* are also shown as labels in Fig. 5. Ozonation was the most efficient process with *TEE* of 503 nmol kJ^{-1}, five-fold higher than Xe/Ce-TiO_2 visible light photocatalysis. In this work, the sample of the ozonation runs was withdrawn once ozone dissolved concentration achieved a plateau at 22 min on stream. Ozonation could lead to even better results in terms of efficiency for lower contact times because, for lower ozone dosages, the amount of transferred energy would be proportionally lower. In any case it is necessary to consider that the minimum ozone dosage would correspond to that required to reach the slow kinetic regime. Therefore, there is no reason for great differences. Concerning irradiation treatments, Xe/Ce-TiO_2 photocatalysis showed a better efficiency than UV and Xe. The data also show a decrease in energy efficiency with treatments time due to the lower reaction rate as pollutant concentration dropped.

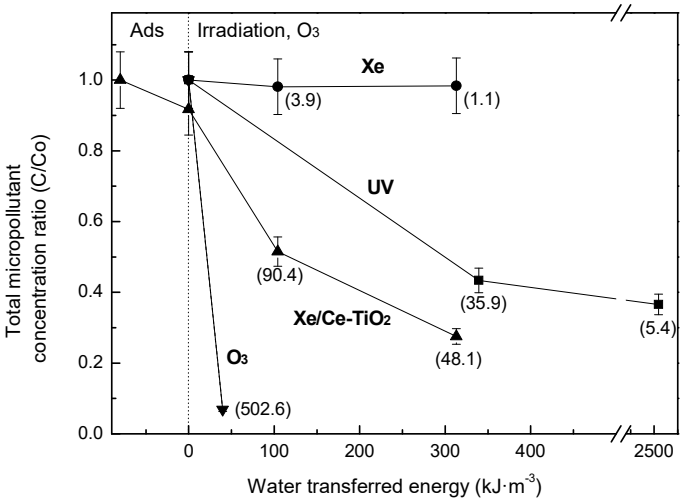

Figure 5. Removal of the total concentration of micropollutants as a function of the energy transferred to water during Xe, Xe/Ce-TiO_2, UV and O_3 treatments. Transferred energy efficiency (TEE, nmol kJ^{-1}) is shown in labels.

Low-pressure mercury vapour lamp irradiation and ozonation are energy-intensive treatments in which electric energy can represent a large fraction of the operating costs. Bolton et al (2001) defined a concept for measuring the energy consumption during the depletion of organic compounds at low concentrations by electrically driven processes called electrical energy per order, E_{EO} (kWh m^{-3} $order^{-1}$). It assumes overall first order kinetic expression and represents the electric energy needed to remove a given pollutant by one order of magnitude in a unit volume of water according to the following equation (written for batch operation):

$$E_{EO} = \frac{P\,t}{V \log\left(\frac{c_i}{c_f}\right)} \qquad (8)$$

P is the electric power, *t* the time, *V* the volume of reaction and c_i and c_f the initial and final concentration respectively.

For solar driven systems the electrical cost of irradiation does not apply because Xe-lamp is assumed to represent a true solar irradiation in a solar collector. In this case, the cost is dominated by the capital investment in the collector and the efficiency is best described in terms of irradiated area. Collector area per order, A_{CO} (m^2 m^{-3} $order^{-1}$), is the collector area needed to obtain one-order-magnitude degradation of a given contaminant (or group of contaminants) per unit of volume receiving "standardized" incident solar fluence rate (E'_{so}) of 1000 W m^{-2} over a period t_o (1h):

$$A_{CO} = \frac{A E'_S\, t}{V \log\left(\frac{c_i}{c_f}\right) E'_{SO}\, t_o} \qquad (9)$$

A is the collector area and E'_s (W m^{-2}) and the average solar fluence rate during the period *t* of the treatment.

Actinometry measurements allowed the determination of the volume based average fluence rate, E'_{vo}:

$$E'_{VO} = \frac{A E'_S}{V} \quad (10)$$

Finally, the volume based average fluence rate, E'_{vo}, can be replaced in Eq. 7 to obtain the collector-area-per-order expression used in this work:

$$A_{CO} = \frac{E'_{VO}\, t}{\log\left(\frac{c_i}{c_f}\right) E'_{SO}\, t_o} \quad (11)$$

Both "figures-of-merit", E_{EO} and A_{CO}, for the treatments used in this work are exposed in Table 3. Ozonation led to E_{EO} of 0.18 kWh m^{-3} $order^{-1}$, which represents a much lower electric consumption than UV irradiation. This consumption agreed with the figures reported by Katsoyiannis et al. (2011), in the 0.0035-0.9 kWh m^{-3} $order^{-1}$ range, and Rodríguez et al. (2012) who obtained 0.03-0.26 kWh m^{-3} $order^{-1}$ for continuous ozonation in a double column arrangement. Most of this variation in ozone efficiency could be explained by the balance between direct and hydroxyl-mediated oxidation processes and the effect of radical scavengers on the latter (Katsoyiannis et al., 2011). Kim and Tanaka (2011) calculated E_{EO} in the 0.03-0.09 kWh m^{-3} $order^{-1}$ range in a process in which they got over 90% removal for most of a set of 37 pharmaceuticals and personal care products. More refractory compounds require higher dosages and consequently other authors found lower efficiencies for the removal of dyes with O_3, O_3/H_2O_2, H_2O_2/UV and TiO_2/UV-A, which were in the 0.23-0.68 kWh m^{-3} $order^{-1}$ range (Arslan et al., 1999; Alaton et al., 2002). For UV treatment, we calculated the required energy considering an electric efficiency of 40% and a quartz transmittance of 92% (254 nm). The obtained E_{EO} was 2.56 ± 1.85 kWh m^{-3} $order^{-1}$, a figure in good agreement with previously reported data for the irradiation of river water and wastewater (Bolton and Stephan, 2002; Benotti et al. 2009; Zoschke et al., 2012). Lower values are associated with treatments in pure water, in which there are less absorbing species (Table S3).

Concerning Xe-lamp irradiated treatments, we assumed the same conditions would stand for a solar collector, with a borosilicate glass transmittance of 86.1% for wavelength range 290-400 nm taken from ASTM G173-03 Reference Solar Spectra and the transmittance data for DURAN glass. The experiments led to collector areas per order of 9.14 ± 5.11 m^2 m^{-3} $order^{-1}$ for Xe irradiation and 0.16 ± 0.03 m^2 m^{-3} $order^{-1}$ for Xe/Ce-TiO_2. These results indicate that Ce-TiO_2 photocatalysis greatly improved the treatment efficiency of solar radiation. The collector area determined in this work for the photocatalytic process was one order-magnitude lower than that found elsewhere for the treatments of oxalic acid, the pesticide carbaryl and certain dyes (Bandala and Estrada, 2007; Rao et al., 2012). This fact could be due to the method of radiation measurement, which in our case was a chemical actinometry instead of radiometer calculations, and also due to the difference in target compounds, which were considerably more refractory for the cited references. (A more detailed reference to results reported in the literature can be found in Table S3.)

4. Conclusions

Ozone treatment achieved a global efficiency over 95% for the removal of the non-polar pollutants studied in this work for 209 ± 37 μM ozone dosage. Particularly HHBC, AHTN, the agrochemicals atrazine, metolachlor, terbutryn, terbuthylazine, chlorpyrifos-ethyl, diazinon, chlorophene, the antiseptic triclosan and the polyaromatic compound pyrene were all removed over 99%.

The irradiation with 254 nm UV reduced the total concentration of the tracked pollutants by an average of 63% with the highest removal for the synthetic musks AHTN and musk ketone and all the herbicides (> 98%) except chlorpyrifos-ethyl (37%).

Visible light Ce-TiO_2 photocatalysis reached ~70% overall removal after 15 minutes of irradiation with the best results for the synthetic musks HHBC, AHTN and musk ketone (removal efficiencies in the 64-85% range). For a significant group of pollutants there was a clear positive relationship between photocatalytic removal efficiency and K_{ow}.

The efficiency in the use of energy was compared using the ratio between pollutant depletion (nmol) and the energy transferred to water (kJ). Ozonation was by far the most efficienct treatment, one order of magnitude ahead of Xe/Ce-TiO_2, which was the irradiation process requiring less energy to remove the same amount of micropollutants.

Expressed in terms of energy per order, ozonation was again preferred, with 0.18 ± 0.06 kWh m^{-3} $order^{-1}$, while UV irradiation at 254 nm consumed 2.56 ± 1.85 kWh m^{-3} $order^{-1}$. Visible light irradiation photocatalysis led to collector areas per order of 0.16 ± 0.03 m^2 m^{-3} $order^{-1}$. The result is lower than other published data for solar degradation of water pollutants, probably reflecting the ability of Ce-TiO_2 to remove non-polar pollutants.

The toxicity of treated wastewater decreased during ozone treatments while irradiation processes led to a toxicity increase due to the accumulation of toxic transformation products, three of which were identified and tracked along the runs. UV irradiation and Xe/Ce-TiO_2 photocatalysis led to a relatively high toxic response for the growth of the green alga *P. subcapitata*.

5. Acknowledgements

This work has been financed by the Dirección General de Universidades e Investigación de la Comunidad de Madrid, Research Network 0505/AMB-0395. One of the authors, JSM, would like to thank the Spanish Ministry

of Education for the award of a FPU grant. Sonia Herrera also acknowledges the "Subprograma de Personal Técnico de Apoyo" of the Spanish Ministry of Science and Technology.

References

Alaton, I.A., Balcioglu, I.A., Bahnemann, D.W., 2002. Advanced oxidation of a reactive dyebath effluent: comparison of O_3, H_2O_2/UV-C and TiO_2/UV-A processes. Water Research 36, 1143-1154.

Allen, J.M., Allen, S.K., Baertschi, S.W., 2000. 2-Nitrobenzaldehyde: a convenient UV-A and UV-B chemical actinometer for drug photostability testing. Journal of Pharmaceutical and Biomedical Analysis 24, 167-178.

Arslan, I., Balcioglu, I.A., Tuhkanen, T., 1999. Advanced oxidation of synthetic dyehouse effluent by O_3, H_2O_2/O_3 and H_2O_2/UV processes. Environmental Technology 20, 921-931.

Bandala, E.R., Estrada, C., 2007. Comparison of solar collection geometries for application to photocatalytic degradation of organic contaminants. Journal of Solar Energy Engineering 129, 22-27.

Beltran, F.J., 2003. Ozone reaction kinetics for water and wastewater systems, Lewis Publishers, CRC Press, Boca Raton, pp. 193-205.

Benotti, M.J., Stanford, B.D., Wert, E.C., Snyder, S.A., 2009. Evaluation of a photocatalytic reactor membrane pilot system for the removal of pharmaceuticals and endocrine disrupting compounds from water. Water Research 43, 1513-1522.

Bester, K., 2004. Retention characteristics and balance assessment for two polycyclic musk fragrances (HHCB and AHTN) in a typical German sewage treatment plant. Chemosphere 57, 863-870.

Boltes, K., Rosal, R., García-Calvo, E., 2012. Toxicity of mixtures of perfluorooctane sulfonic acid with chlorinated chemicals and lipid regulators. Chemosphere 86, 24–29.

Bolton, J.R., Stefan, M.I., 2002. Fundamental photochemical approach to the concepts of fluence (UV dose) and electrical energy efficiency in photochemical degradation reactions. Research on Chemical Intermediates 28, 857-870.

Bolton, J.R., Bircher, K.G., Tumas, W., Tolman, C.A., 2001. Figures-of-merit for the technical development and application of advanced oxidation technologies for both electric-and solar-driven systems (IUPAC Technical Report). Pure and Applied Chemistry 73, 627-638.

Champagne, P., 2008. Personal care products. In: Alok Bhandari, Rao Y. Surampalli, Craig D. Adams, Pascale Champagne, Say Kee Ong, and R. D. Tyagi (Eds.), Contaminants of Emerging Environmental Concern. American Society of Civil Engineers, Reston, pp. 86-140.

D'Oliveira, J.C., Minero, C., Pelizzetti, E. and Pichat, P., 1993. Photodegradation of dichlorophenols and trichlorophenols in TiO_2 aqueous suspensions: kinetic effects of the positions of the Cl atoms and identification of the intermediates. Journal of Photochemistry and Photobiology A: Chemistry 72, 261-267.

Esplugas, S., Bila, D.M., Krause, L.G.T., Dezotti, M., 2007. Ozonation and advanced oxidation technologies to remove endocrine disrupting chemicals (EDCs) and pharmaceuticals and personal care products (PPCPs) in water effluents. Journal of Hazardous Materials 149, 631-642.

Friedmann, D., Mendive, C., Bahnemann, D., 2010. TiO2 for water treatment: Parameters affecting the kinetics and mechanisms of photocatalysis. Applied Catalysis B Environmental 99, 398-406.

Gatermann, R., Hühnerfuss, H., Rimkus, G., Attar, A., Kettrup, A, 1998. Occurrence of musk xylene and musk ketone metabolites in the aquatic environment. Chemosphere 36, 2535-2547.

Gómez, M.J., Herrera, S., Solé, D., García-Calvo, E., Fernández-Alba, A.R., 2011. Automatic searching and evaluation of priority and emerging contaminants in wastewater and river water by stir bar sorptive extraction followed by comprehensive two-dimensional gas chromatography-time-of-flight mass spectrometry. Analytical Chemistry 83, 2638-2647.

Gómez, M.J., Herrera, S., Solé, D., García-Calvo, E., Fernández-Alba, A.R., 2012. Spatio-temporal evaluation of organic contaminants and their transformation products along a river basin affected by urban, agricultural and industrial pollution. Science of the Total Environment 420, 134-145.

Gómez-Ramos, M.M., Mezcua, M., Agüera, A., FernándezAlba, A.R., Gonzalo, S., Rodríguez, A., Rosal, R., 2011. Chemical and toxicological evolution of the antibiotic sulfamethoxazole under ozone treatment in water solution. J. Hazard. Mater. 192, 18-25.

International Organization for Standardization. Water Quality-Determination of the Inhibitory Effect of Water Samples on the Light Emission of Vibrio fischeri (Luminescent Bacteria Test). ISO 11348-3 revised version, Geneva, Switzerland, 2007.

Herrera, S., Hernando, M.D., Gómez, M.J., Santiago-Morales, J., Rosal, R., Fernández-Alba, A.R., 2013. Investigation of Galaxolide degradation products generated under oxidative and irradiation processes by liquid chromatography/hybrid quadrupole time-of-flight mass spectrometry and comprehensive two-dimensional gas chromatography/time-of-flight mass spectrometry. Rapid Commun. Mass Sp. 27, 1237-1250.

Huijbregts, M.A.J., Thissen, U., Guinée, J.B., Jager, T., Kalf, D., van de Meent, D., Ragas, A.M., Sleeswijk, A.W., Reijnders, L., 2010. Priority assessment of toxic substances in life cycle assessment. Part I: Calculation of toxicity potentials for substances with the nested multi-media fate, exposure and effects model USES-LCA. Chemosphere 41, 541–573.

Kümmerer, K., 2011. Emerging Contaminants, In: Peter Wilderer (Ed.), Treatise on Water Science, Elsevier, Oxford, pp. 69-87.

Katsoyiannis, I.A., Canonica, S., von Gunten, U., 2011. Efficiency and energy requirements for the transformation of organic micropollutants by ozone, O_3/H_2O_2 and UV/H_2O_2. Water Research 45, 3811-3822.

Kim, I., Tanaka, H., 2011. Energy Consumption for PPCPs Removal by O_3 and O_3/UV. Ozone Science & Engineering 33, 150-157.

Kuhlich, P., Göstl, R., Teichert, P., Piechotta, C., Nehls, I., 2011. Transformations of polycyclic musks AHTN and HHCB upon disinfection with hypochlorite: two new chlorinated disinfection by-products (CDBP) of AHTN

and a possible source for HHCB-lactone. Anal. Bioanal. Chem. 399, 3579-3588.
Krichevskaya, M., Klauson, D., Portjanskaja, E., Preis, S., 2011. The Cost evaluation of advanced oxidation processes in laboratory and pilot-scale experiments. Ozone Science & Engineering 33, 211-223.
Lam, M.W., Tantuco, K., Mabury, S.A., 2003. PhotoFate: A new approach in accounting for the contribution of indirect photolysis of pesticides and pharmaceuticals in surface waters. Environ. Sci. Technol. 37,899-907.
Lindsey, M. E., Tarr, M. A., 2000. Inhibition of hydroxyl radical reaction with aromatics by dissolved natural organic matter. Environ. Sci. Technol., 34, 444–449.
Miège, C., Peretti, A., Labadie, P., Budzinski, H., Le Bizec, B., Vorkamp, K., Tronczyński, J., Persat, H., Coquery, M., Babut, M., 2012. Occurrence of priority and emerging organic compounds in fishes from the Rhone River (France). Analytical and Bioanalytical Chemistry 404, 2721-2735.
Muñoz, I., Rodríguez, A., Rosal, R., Fernández-Alba, A.R., 2009. Life cycle assessment of urban wastewater reuse with ozonation as tertiary treatment: a focus on toxicity-related impacts. Science of the Total Environment 407, 1245-1256.
Nicole, I., Delaat, J., Dore, M., Duguet, J.P., Bonnel, C., 1990. Use of UV-radiation in water treatment. Measurement of photonic flux by hydrogen-peroxide actinometry. Water Research 24, 157-168.
OECD, Test No. 201: Freshwater Alga and Cyanobacteria, Growth Inhibition Test, OECD Guidelines for the Testing of Chemicals, Section 2, OECD Publishing, 2011.
OECD, Test No. 202: Daphnia sp. Acute Immobilisation Test, OECD Guidelines for the Testing of Chemicals, Section 2, OECD Publishing, 2004.
Rao, N.N., Chaturvedi, V., Li Puma, G., 2012. Novel pebble bed photocatalytic reactor for solar treatment of textile wastewater. Chemical Engineering Journal 184, 90-97.
Rodea-Palomares, I., Petre, A.L., Boltes, K., Leganés, F., Perdigón-Melón, J.A., Rosal, R., Fernández-Piñas, F., 2010. Application of the combination index (CI)-isobologram equation to study the toxicological interactions of lipid regulators in two aquatic bioluminescent organisms. Water Research 44, 427-438.
Rodríguez, A., Muñoz, I., Perdigón-Melón, J.A., Carbajo, J.B., Martínez, M.J., Fernández-Alba, A.R., García-Calvo, E., Rosal, R., 2012. Environmental optimization of continuous flow ozonation for urban wastewater reclamation. Science of the Total Environment 437, 68-75.
Rosal, R., Rodríguez, A., Gonzalo, M.S., García-Calvo, E., 2008. Catalytic ozonation of naproxen and carbamazepine on titanium dioxide. Applied Catalysis B Environmental 84, 48-57.
Rosal, R., Gonzalo, M.S., Boltes, K., León, P., Vaquero, J.J., García-Calvo, E., 2009. Identification of intermediates and assessment of ecotoxicity in the oxidation products generated during the ozonation of clofibric acid. Journal of Hazardous Materials 172, 1061-1068.
Rosal, R., Rodríguez, A., Perdigón-Melón, J.A., Petre, A., García-Calvo, E., Gómez, M.J., Agüera, A., Fernández-Alba, A.R., 2010. Occurrence of emerging pollutants in urban wastewater and their removal through biological treatment followed by ozonation. Water Research 44, 578-588.
Santiago-Morales, J., Gómez, M.J., Herrera, S., Fernández-Alba, A.R., García-Calvo, E., Rosal, R., 2012. Oxidative and photochemical processes for the removal of galaxolide and tonalide from wastewater. Water Research 46, 4435-4447.
Santiago-Morales, J., Agüera, A., Gómez, M.M., Fernández-Alba, A.R., Giménez, J., Esplugas, S., Rosal, R., 2013. Transformation products and reaction kinetics in simulated solar light photocatalytic degradation of propranolol using Ce-doped TiO_2. Applied Catalysis B Environmental 129, 13-29.
Shang, N.C., Yu, Y.H., Ma, H.W., Chang, C.H. , Liou, M.L., 2006. Toxicity measurements in aqueous solution during ozonation of mono-chlorophenols. Journal of environmental management 78, 216-222.
Snyder, S.A., Wert, E.C., Rexing, D.J., Zegers, R.E., Drury, D.D., 2006. Ozone oxidation of endocrine disruptors and pharmaceuticals in surface water and wastewater. Ozone Science & Engineering 28, 445-460.
Tanaka, K., Reddy, K., 2002. Photodegradation of phenoxyacetic acid and carbamate pesticides on TiO2. Applied Catalysis B: Environmental 39, 305-310.
Valdersnes, S., Kallenborn, R., Sydnes, L.K., 2006. Identification of several Tonalide® transformation products in the environment. International Journal of Environmental Analytical Chemistry 86, 461-471.
Van der Oost, R., Beyer, J., Vermeulen, N.P.E., 2003. Fish bioaccumulation and biomarkers in environmental risk assessment: a review. Environmental Toxicology and Pharmacology 13, 57-149.
Werner, J.J., McNeill, K., Arnold, W.A., 2005. Environmental photodegradation of mefenamic acid. Chemosphere 58, 1339-1346.
Zhang, Q.H., Wang, X.C., Xiong, J.Q., Chen, R., Cao, B., 2010. Application of life cycle assessment for an evaluation of wastewater treatment and reuse project—case study of Xi'an. Bioresource Technology 101, 1421–1425.
Zoschke, K., Dietrich, N., Börnick, H., Worch, E., 2012. UV-based advanced oxidation processes for the treatment of odour compounds: Efficiency and by-product formation. Water Research 46, 5365–5373

SUPPLEMENTARY MATERIAL

Energy efficiency for the removal of non-polar pollutants during ultraviolet irradiation, visible light photocatalysis and ozonation of a wastewater effluent

Javier Santiago-Morales[1], María José Gómez[2,3], Sonia Herrera[2,3], Amadeo R. Fernández-Alba[2,3], Eloy García-Calvo[1,2], Roberto Rosal[1,2,✉]

[1] Department of Chemical Engineering, University of Alcalá, 28871 Alcalá de Henares, Madrid, Spain
[2] Advanced Study Institute of Madrid, IMDEA Agua, Parque Científico Tecnológico, 28805 Alcalá de Henares, Madrid, Spain.

[3] Pesticide Residue Research Group, Department of Hydrogeology and Analytical Chemistry, University of Almería, 04120, Spain.

Table S1. Properties of micropollutants

Table S2. Properties of micropollutants (continued)

Table S3. Electrical energy per order per order, E_{EO} (kWh m^{-3} order) and collector area per order, A_{CO} (m^2 m^{-3} $order^{-1}$) in the literature.

References

✉ corresponding author: roberto.rosal@uah.es

Table S1. Properties of micropollutants

Function	Substance	CAS No.	Molecular formula	pK_a	Log K_{ow}[d]	Log D_{ow}[e]
UV filter / sunscreen	2-Ethylhexyl trans-4-methoxycinnamate	5466-77-3	$C_{18}H_{26}O_3$	- [a]	5.8	5.8
UV filter / sunscreen	Oxybenzone	131-57-7	$C_{14}H_{12}O_3$	9.7 [a]	3.79	3.79
Synthetic musk	Galaxolide (HHBC)	1222-05-5	$C_{18}H_{26}O$	- [b]	5.9	5.90
Synthetic musk	Musk ketone	81-14-1	$C_{14}H_{18}N_2O_5$	- [a]	4.3	4.30
Synthetic musk	Tonalide (AHTN)	21145-77-7	$C_{18}H_{26}O$	- [b]	5.7	5.70
Food additive / antioxidant	Butyl hydroxytoluene (BHT)	128-27-0	$C_{15}H_{24}O$	12.23 [c]	5.1	5.10
Herbicide	Atrazine [PH]	1912-24-9	$C_8H_{14}ClN_5$	12.3 [a]	2.61	2.61
Herbicide	Metolachlor	51218-45-2	$C_{15}H_{22}ClNO_2$	12.55 [a]	3.13	3.13
Herbicide	Terbutryn [PH]	886-50-0	$C_{10}H_{19}N_5S$	9.7 [c]	3.74	3.74
Herbicide	Terbuthylazine	5915-41-3	$C_9H_{16}ClN_5$	12 [c]	3.21	3.21
Insecticide	Chlorpyrifos-ethyl [PH]	2921-88-2	$C_9H_{11}Cl_3NO_3PS$	- [a]	4.96	4.96
Insecticide	Diazinon	333-41-5	$C_{12}H_{21}N_2O_3PS$	12.4 [a]	3.81	3.81
Disinfectant	Chlorophene	120-32-1	$C_{13}H_{11}ClO$	9.6 [a]	3.6	3.60
Antiseptic	Triclosan	3380-34-5	$C_{12}H_7Cl_3O_2$	7.8 [b]	4.76	4.64
Combustion by-product	Pyrene [PHS]	129-00-0	$C_{16}H_{10}$	-	4.88	4.88
Combustion by-product	Phenanthrene [PHS]	85-01-8	$C_{14}H_{10}$	-	4.46	4.46

a) ACD/Ilab Web service Advanced_Chemistry_Development_Inc.; b) Rosal et al. 2010; c) U.S_National_Library_of_Medicine; d) Gómez et al. 2011; e) log D_{ow}: logarithm of pH-dependent or apparent octanol–water distribution coefficient, D_{ow} [for basic compounds, this coefficient can be determined by the following equation using pK_a for the corresponding conjugate acid (Rosal et al., 2010): $Dow = \frac{Kow}{1+10^{pKa-pH}}$] ; PS: priority substance; PHS: priority hazardous substance. PS and PHS are according to the Proposal COM 2011,876 final 31.1.2012 of European Parliament and Council

Table S2. Properties of micropollutants (continued)

Substance	Spectrum range	$\phi_{254\ nm}$ ($\times10^{-3}$)	$\varepsilon_{254\ nm}$ ($M^{-1}\ cm^{-1}$)	$\phi_{>290\ nm}$ [c] ($\times10^{-3}$)	$\varepsilon_{>290\ nm}$ [c] ($M^{-1}\ cm^{-1}$)	k_{O3} ($M^{-1}\ s^{-1}$)	k_{OH} ($\times10^{9}\ M^{-1}\ s^{-1}$)
2-Ethylhexyl trans-4-methoxycinnamate	< 340 nm [1]	-	1550 [11]	-	25300 [11]	-	-
Oxybenzone	< 400 nm [2]	0.13 [a]	6653 [12]	0.13 [12]	5900 [12]	$5.0\cdot10^{6}$ [23]	-
Galaxolide (HHBC)	< 300 nm [b]	-	486[b]	-	20.4[b]	140 [24]	4.72 [32]
Musk ketone	-	-	-	-	-	-	1.49 [33]
Tonalide (AHTN)	< 340 nm [b]	120 [a]	12613[b]	120 [20]	849 [b]	8 [24]	5.00 [24]
Butyl hydroxytoluene (BHT)	< 295 nm [3]	-	316 [3]	-	39.8 [3]	-	-
Atrazine	< 290 nm [b]	53 [12]	3768 [12]	53 [a]	0	6 [25]	2.54 [35]
Metolachlor	< 305 nm [4]	302 [15]	615 [4]	302 [a]	9.6 [4]	1.11 [26]	6.70 [26]
Terbutryn	< 290 nm [5]	79 [16]	4210 [5]	79 [a]	0	-	-
Terbutylazine	< 290 nm [6]	94 [17]	3830 [17]	94 [a]	0	8.9 [28]	2.80 [27]
Chlorpyrifos-ethyl	< 310 nm [7]	16 [18]	900 [18]	52 [18]	330 [18]	-	4.90 [35]
Diazinon	< 320nm [8]	86 [8]	3558 [4]	58 [8]	89 [4]	1602 [28]	9.00 [8]
Chlorophene	< 300 nm [9] (based on dichlorophene)	-	-	-	-	-	10.0 [29]
Triclosan	< 300 nm (acid form) < 320 nm (basic form) [10]	480 [22]	3300 [10]	740 [21]	1500 [10]	$1.81\cdot10^{8}$ [30]	5.40 [31]
Pyrene	< 384 nm [14]	3.83 [39]	13461 [14]	2.1 [14]	7179 [14]	$3.60\cdot10^{4}$ [38]	10.0 [36]
Phenanthrene	< 355 nm [14]	6.9 [19]	45753 [14]	3.5 [14]	1222 [14]	$1.0\cdot10^{4}$ [38]	13.4 [37]

1) Kikuchi et al., 2010; 2) Serpone et al., 2002; 3) NIST, 2012; 4) Feigenbrugel et al., 2005; 5) Gonzalez et al., 2007; 6) Palm et al., 1997; 7) Moffat et al. 2011; 8) Shemer and Linden, 2006; 9) Ghauch and Tuqan, 2009; 10) Lindström et al., 2002; 11) Panday, 2002; 12) Serpone et al., 2002;; 12) Santiago et al., 2011;; 14) Ram and Anastasio, 2009; 15) Wu et al., 2007; 16) Zwiener et al., 1995; 17) Nick et al., 1992; 18) Wan et al., 1994; 19) Beltrán et al., 1995; 20) European Union, 2008; 21) Latch et al., 2003; 22) Chung et al., 2007; 23) Huber et al., 2003; 24) Nöthe et al., 2007; 25) Acero et al., 2000; 26) Acero et al., 2003; 27) Camel and Bermond, 1998; 28) Ku et al., 1998; 29) Sires et al., 2007; 30) Suarez et al., 2007; 31) Latch et al., 2009; 32) Ward, 2010; 33) Hirsch, 2011; 35) Balci et al., 2009; 35) Wu and Linden, 2010; 36) Haag and Yao, 1992; 37) Beltrán, 2003; 38) Trapido et al., 1995; 39) Lehto et al., 2000; a) Quantum yield 254 nm ≈ Quantum yield >290 nm; b) Measured in this work. c) $\phi_{>290\ nm}$ and $\varepsilon_{>290\ nm}$ corresponds to averaged values between 290 nm and the maximum absorbance wavelength.

Table S3 Electrical energy per order per order, E_{EO} (kWh m^{-3} order) and collector area per order, A_{CO} (m^2 m^{-3} $order^{-1}$) in the literature.

	Treatment	This work	Literature value	Conditions	References
E_{EO} (kWh m^{-3} $order^{-1}$)	UV	2.56 ± 1.85	0.2[a] to 1.3[b]	[a]Ultrapure water, [b]Raw water 2-methyl isoborneol and geosmin	(Zoschke et al., 2012)
			0.628	Atrazine (~100 ppb), MQ water	(Bolton and Stefan, 2002)
			0.3-0.5	Deionised water 0.001 mM N-nitrosodimethylamine	(Stefan and Bolton, 2002)
			~1-50	Atenolol–TCEP (ng L^{-1}) in river water	(Benotti et al., 2009)
	O_3	0.18	0.0035 (SMX) 0.9 (NDMA)	Sulfamethoxazole [k_{O3} $2.5 \cdot 10^6$ M^{-1} s^{-1} (pH 7), k_{OH} $5 \cdot 10^9$ M^{-1} s^{-1}] N-nitrosodimethylamine [k_{O3} 0.052 M^{-1} s^{-1}, k_{OH} $4.5 \cdot 10^8$ M^{-1} s^{-1}]	(Katsoyiannis et al., 2011)
			0.03-0.09	Number of removed PPCPs > 90% / total number of PPCP 24/37 - 35/37	(Kim and Tanaka, 2011)
			0.684	Dyebath effluent	(Alaton et al., 2002)
			0.23	Dyehouse, pH 11	(Arslan et al., 1999)
			0.03-0.26	Two ozonation columns, 0.30 L min^{-1}, 90% removal	(Rodríguez et al., 2012)
A_{CO} (m^2 m^{-3} $order^{-1}$)	Xe	9.14 ± 5.11	NF	NF	NF
	Xe-$CeTiO_2$	0.16 ± 0.03	12-37.5 8.7-5.5	Oxalic acid degradation (10 mM): PTC-CPC, 50 mg/L TiO_2 PTC-CPC,1 g/L TiO_2	(Bandala and Estrada, 2007)
			14 9.6	Carbaryl degradation (0.25mM): PTC 0.05g/L TiO_2 CPC 0.5g/L TiO_2	
			8.6-11.2	Pebble bet, Different Dyes, 20-50 mg/L deionised water	(Rao et al., 2012)

PTC: parabolic trough collector
CPC Concentrating Parabolic Collector)
NF: not found

References

Acero, J.L., Stemmler, K., von Gunten, U., 2000. Degradation kinetics of atrazine and its degradation products with ozone and OH radicals: a predictive tool for drinking water treatment. Environmental Science & Technology 34, 591-597.

Acero, J.L., Benitez, F.J., Real, F.J., Maya, C., 2003. Oxidation of acetamide herbicides in natural waters by ozone and by the combination of ozone/hydrogen peroxide: Kinetic study and process modeling. Industrial & Engineering Chemistry Research 42, 5762-5769.

Advanced_Chemistry_Development_Inc.,PhysChem Properties in: ACD/I-Lab, ilab.acdlabs.com, 2012/09

Alaton, I.A., Balcioglu, I.A., Bahnemann, D.W., 2002. Advanced oxidation of a reactive dyebath effluent: comparison of O_3, H_2O_2/UV-C and TiO_2/UV-A processes. Water Research 36, 1143-1154.

Arslan, I., Balcioglu, I.A., Tuhkanen, T., 1999. Advanced oxidation of synthetic dyehouse effluent by O_3, H_2O_2/O_3 and H_2O_2/UV processes. Environmental Technology 20, 921-931.

Balci, B., Oturan, N., Cherrier, R., Oturan, M.A., 2009. Degradation of atrazine in aqueous medium by electrocatalytically generated hydroxyl radicals. A kinetic and mechanistic study. Water Research 43, 1924-1934.

Bandala, E.R., Estrada, C., 2007. Comparison of solar collection geometries for application to photocatalytic degradation of organic contaminants. Journal of Solar Energy Engineering 129, 22-26.

Beltrán, F.J., Ovejero, G., Garcia-Araya, J.F., Rivas, J., 1995. Oxidation of polynuclear aromatic hydrocarbons in water. 2. UV radiation and ozonation in the presence of UV radiation. Industrial & Engineering Chemistry Research 34, 1607-1615.

Beltrán, F.J. (2003) Ozone reaction kinetics for water and wastewater systems, Lewis Publishers, CRC Press, Boca Raton.

Benotti, M.J., Stanford, B.D., Wert, E.C., Snyder, S.A., 2009. Evaluation of a photocatalytic reactor membrane pilot system for the removal of pharmaceuticals and endocrine disrupting compounds from water. Water research 43, 1513-1522.

Bolton, J.R., Stefan, M.I., 2002. Fundamental photochemical approach to the concepts of fluence (UV dose) and electrical energy efficiency in photochemical degradation reactions. Research on Chemical Intermediates 28, 857-870.

Camel, V., Bermond, A., 1998. The use of ozone and associated oxidation processes in drinking water treatment. Water Research 32, 3208-3222.

European Union, 2008. European Union Risk Assessment Report. 1-(5,6,7,8-Tetrahydro-3,5,5,6,8,8-hexamethyl-2-naphtyl)ethan-1-one (AHTN) , European Communities, Luxembourg.

Feigenbrugel, V., Loew, C., Calvé, S.L., Mirabel, P., 2005. Near-UV molar absorptivities of acetone, alachlor, metolachlor, diazinon and dichlorvos in aqueous solution. Journal of Photochemistry and Photobiology A: Chemistry 174, 76-81.

Ghauch, A., Tuqan, A., 2009. Reductive destruction and decontamination of aqueous solutions of chlorinated antimicrobial agent using bimetallic systems. Journal of hazardous materials 164, 665-674.

Gomez, M.J., Herrera, S., Sole, D., Garcia-Calvo, E., Fernandez-Alba, A.R., 2011. Automatic Searching and Evaluation of Priority and Emerging Contaminants in Wastewater and River Water by Stir Bar Sorptive Extraction followed by Comprehensive Two-Dimensional Gas Chromatography-Time-of-Flight Mass Spectrometry. Analytical Chemistry 83, 2638-2647.

Gonzalez, C., Touraud, E., Spinelli, S., Thomas, O., 2007. Organic Constituents in: Olivier Thomas and Christopher Burgess (Eds.) UV-visible Spectrophotometry of Water and Wastewater, Elsevier Science Limited, Amsterdam

Haag, W.R., Yao, C.C.D., 1992. Rate constants for reaction of hydroxyl radicals with several drinking water contaminants. Environmental Science & Technology 26, 1005-1013.

Hirsch, C.M., 2011. The removal of synthetic musks and other personal care product chemicals from reclaimed wastewater using radical reactions, M.Sc. Thesis, California State University, Long Beach.

Huber, M.M., Canonica, S., Park, G.Y., von Gunten, U., 2003. Oxidation of pharmaceuticals during ozonation and advanced oxidation processes. Environmental Science & Technology 37, 1016-1024.

Katsoyiannis, I.A., Canonica, S., von Gunten, U., 2011. Efficiency and energy requirements for the transformation of organic micropollutants by ozone, O_3/H_2O_2 and UV/H_2O_2. Water Research 45, 3811-3822.

Kikuchi, A., Yukimaru, S., Oguchi, N., Miyazawa, K., Yagi, M., 2010. Excited triplet state of a UV-B absorber, octyl methoxycinnamate. Chemistry Letters 39, 633-635.

Kim, I., Tanaka, H., 2011. Energy consumption for PPCPs removal by O_3 and O_3/UV. Ozone Science & Engineering 33, 150-157.

Ku, Y., Chang, J.L., Shen, Y.S., Lin, S.Y., 1998. Decomposition of diazinon in aqueous solution by ozonation. Water Research 32, 1957-1963.

Latch, D.E., Packer, J.L., Arnold, W.A., McNeill, K., 2003. Photochemical conversion of triclosan to 2, 8-dichlorodibenzo-p-dioxin in aqueous solution. Journal of Photochemistry and Photobiology A: Chemistry 158, 63-66.

Latch, D.E., Packer, J.L., Stender, B.L., Van Overbeke, J., Arnold, W.A., McNeill, K., 2009. Aqueous photochemistry of triclosan: formation of 2, 4-dichlorophenol, 2, 8-dichlorodibenzo-p-dioxin, and oligomerization products. Environmental Toxicology and Chemistry 24, 517-525.

Lehto, K.M., Vuorimaa, E., Lemmetyinen, H., 2000. Photolysis of polycyclic aromatic hydrocarbons (PAHs) in dilute aqueous solutions detected by fluorescence. Journal of Photochemistry and Photobiology A: Chemistry 136, 53-60.

Lindström, A., Buerge, I.J., Poiger, T., Bergqvist, P.A., Müller, M.D., Buser, H.R., 2002. Occurrence and environmental behavior of the bactericide triclosan and its methyl derivative in surface waters and in wastewater. Environmental Science & Technology 36, 2322-2329.

Moffat, A., Osselton, D., Widdop, B. and Galichet, L.Y., 2011. Chlorpyrifos in: Analysis of Drugs and Poisons, http://mtnviewfarm.net/drugs-poisons-0356.html, 12/2012

Nick, K., Schöler, H., Mark, G., Söylemez, T., Akhlaq, M., Schuchmann, H., von Sonntag, C., 1992. Degradation of some triazine herbicides by UV radiation such as used in the UV disinfection of drinking water. Aqua- Journal of Water Supply: Research and Technology 41, 82-87.

NIST, N.I.o.S.a.T.,NIST chemistry webbook, NIST standard reference database number 69, U.S.Secretary of Commerce on behalf of the United States of America, http://webbook.nist.gov/chemistry/, 12/2012

Nöthe, T., Hartmann, D., Fahlenkamp, H., Von Sonntag, C., von Sonntag, J., 2007. Elimination of the musk fragrances galaxolide and tonalide from wastewater by ozonation and concomitant stripping. Water Science and Technology 55, 287-292.

Palm, W.U., Elend, M., Krueger, H.U., Zetzsch, C., 1997. OH radical reactivity of airborne terbuthylazine adsorbed on inert aerosol. Environmental Science & Technology 31, 3389-3396.

Panday, R. (2002) A photochemical investigation of two sunscreen absorbers in a polar and a non-polar medium. M.Sc. Thesis, University of Natal, Durban.
Ram, K., Anastasio, C., 2009. Photochemistry of phenanthrene, pyrene, and fluoranthene in ice and snow. Atmospheric Environment 43, 2252-2259.
Rao, N.N., Chaturvedi, V., Li Puma, G., 2012. Novel pebble bed photocatalytic reactor for solar treatment of textile wastewater. Chemical Engineering Journal 184, 90-97.
Rodríguez, A., Muñoz, I., Perdigón-Melón, J.A., Carbajo, J.B., Martínez, M.J., Fernández-Alba, A.R., García-Calvo, E., Rosal, R., 2012. Environmental optimization of continuous flow ozonation for urban wastewater reclamation. Science of the Total Environment 437, 68-75.
Rosal, R., Rodríguez, A., Perdigón-Melón, J.A., Petre, A., García-Calvo, E., Gómez, M.J., Agüera, A., Fernández-Alba, A.R., 2010. Occurrence of emerging pollutants in urban wastewater and their removal through biological treatment followed by ozonation. Water Research 44, 578-588.
Sanches, S., Leitão, C., Penetra, A., Cardoso, V., Ferreira, E., Benoliel, M., Crespo, M., Pereira, V., 2011. Direct photolysis of polycyclic aromatic hydrocarbons in drinking water sources. Journal of hazardous materials 192, 1458-1465.
Santiago, J., Agüera, A., del Mar Gómez-Ramos, M., Fernández Alba, A.R., García-Calvo, E., Rosal, R., 2011. Oxidation by-products and ecotoxicity assessment during the photodegradation of fenofibric acid in aqueous solution with UV and UV/H_2O_2. Journal of hazardous materials 194, 30-41.
Serpone, N., Salinaro, A., Emeline, A.V., Horikoshi, S., Hidaka, H., Zhao, J., 2002. An in vitro systematic spectroscopic examination of the photostabilities of a random set of commercial sunscreen lotions and their chemical UVB/UVA active agents. Photochemical & Photobiological Sciences 1, 970-981.
Shemer, H., Linden, K.G., 2006. Degradation and by-product formation of diazinon in water during UV and UV/H_2O_2 treatment. Journal of hazardous materials 136, 553-559.
Sires, I., Garrido, J.A., Rodriguez, R.M., Brillas, E., Oturan, N., Oturan, M.A., 2007. Catalytic behavior of the Fe^{3+}/Fe^{2+} system in the electro-Fenton degradation of the antimicrobial chlorophene. Applied Catalysis B: Environmental 72, 382-394.
Stefan, M.I., Bolton, J.R., 2002. UV direct photolysis of N-nitrosodimethylamine (NDMA): kinetic and product study. Helvetica Chimica Acta 85, 1416-1426.
Suarez, S., Dodd, M.C., Omil, F., von Gunten, U., 2007. Kinetics of triclosan oxidation by aqueous ozone and consequent loss of antibacterial activity: relevance to municipal wastewater ozonation. Water Research 41, 2481-2490.
Trapido, M., Veressinina, Y., Munter, R., 1995. Ozonation and advanced oxidation processes of polycyclic aromatic hydrocarbons in aqueous solutions-a kinetic study. Environmental Technology 16, 729-740.
U.S_National_Library_of_Medicine,ChemIDplus Advanced, http://chem.sis.nlm.nih.gov/chemidplus/, 12/2012
Wan, H.B., Wong, M.K., Mok, C.Y., 1994. Comparative study on the quantum yields of direct photolysis of organophosphorus pesticides in aqueous solution. Journal of Agricultural and Food Chemistry 42, 2625-2630.
Ward, C.P., 2010. Direct and indirect photochemical degradation of two polycyclic musk fragrances and two polycyclic aromatic hydrocarbons in natural waters, M.Sc. Thesis, The Ohio State University.
Chung, P.W.W., Rafqah, S., Voyard, G., Sarakha, M., 2007. Photochemical behaviour of triclosan in aqueous solutions: kinetic and analytical studies. Journal of Photochemistry and Photobiology A: Chemistry 191, 201-208.

Wu, C., Shemer, H., Linden, K.G., 2007. Photodegradation of metolachlor applying UV and UV/H_2O_2. Journal of Agricultural and Food Chemistry 55, 4059-4065.
Wu, C., Linden, K.G., 2010. Phototransformation of selected organophosphorus pesticides: Roles of hydroxyl and carbonate radicals. Water Research 44, 3585-3594.
Zoschke, K., Dietrich, N., Börnick, H., Worch, E., 2012. UV-based advanced oxidation processes for the treatment of odour compounds: Efficiency and by-product formation. Water Research 46, 5365-3573.
Zwiener, C., Weil, L. , Niessner, R., 1995. UV-und UV/Ozon-Abbau von Triazinherbiziden in einer Pilotanlage-Bestimmung von Ratenkonstanten und Quantenausbeuten der UV-Photolyse. Vom Wasser 84, 47-60.